Journal of Cellular Biochemistry 85:747–761 (2002)

Characterization of a TM-4 Type Tropomyosin That Is Essential for Myofibrillogenesis and Contractile Activity in Embryonic Hearts of the Mexican Axolotl

Belinda J. Spinner,[2] Robert W. Zajdel,[2] Matthew D. McLean,[2] Christopher R. Denz,[1] Syamalima Dube,[1] Sonali Mehta,[1] Aruna Choudhury,[2] Masako Nakatsugawa,[2] Nancy Dobbins,[2] Larry F. Lemanski,[3] and Dipak K. Dube[1,2]*

[1]Department of Medicine, Upstate Medical University, 750 East Adams Street, Syracuse, New York 13210
[2]Department of Cell and Developmental Biology, Upstate Medical University, 750 East Adams Street, Syracuse, New York 13210
[3]Department of Medical Physiology, Texas A&M University, College Station, Texas 77843

Abstract A striated muscle isoform of a Tropomyosin (TM-4) gene was characterized and found to be necessary for contractile function in embryonic heart. The full-length clone of this isoform was isolated from the Mexican axolotl (*Ambystoma mexicanum*) and named Axolotl Tropomyosin Cardiac-3 (ATmC-3). The gene encoded a cardiac-specific tropomyosin protein with 284 amino acid residues that demonstrated high homology to the *Xenopus* cardiac TM-4 type tropomyosin. Northern blot analysis indicates a transcript of ~1.25 kb in size. RT-PCR and in situ hybridization demonstrated that this isoform is predominantly in cardiac tissue. Our laboratory uses an animal model that carries a cardiac lethal mutation (gene c), this mutation results in a greatly diminished level of tropomyosin protein in the ventricle. Transfection of ATmC-3 DNA into mutant hearts increased tropomyosin levels and promoted myofibrillogenesis. ATmC-3 expression was blocked in normal hearts by transfection of exon-specific anti-sense oligonucleotide (AS-ODN). RT-PCR confirmed lower transcript expression of ATmC-3 and in vitro analysis confirmed the specificity of the ATmC-3 exon 2 anti-sense oligonucleotide. These AS-ODN treated hearts also had a disruption of myofibril organization and disruption of synchronous contractions. These results demonstrated that a striated muscle isoform of the TM-4 gene was expressed embryonically and was necessary for normal structure and function of the ventricle. J. Cell. Biochem. 85:747–761, 2002.

Key words: oligonucleotide; transfection; tropomyosin isoforms; nonmuscle tropomyosin; alternative splicing

Diverse expression of tropomyosin isoforms in various tissues is a complex process involving different genes, promoters, or alternative splicing [Helfman et al., 1986; Wieczorek et al., 1988; Cho and Hitchcock-DeGregori, 1991; Pittenger et al., 1994; Lin et al., 1997]. These diverse isoforms have as yet unknown control mechanisms that regulate developmental and tissue specific expression. Once expressed, isoform-specific interactions with complementary proteins, such as actin, may also have important implications for structure and func-

Abbreviations: aa, amino acids; AS-ODN, anti-sense oligonucleotide; ATmC-3, axolotl tropomyosin cardiac-3; RT-PCR, reverse transcriptase-polymerase chain reaction; bp, base pair; Ca, cardiac; cDNA, complementary DNA; FS-ODN, fluorescence (cein) sense-oligonucleotide; GCG, genetic computer group (Madison, WI, USA); h, human; kb, kilobase(s); NM, nonmuscle; nt, nucleotide(s); RACE, rapid amplification of cDNA ends; SDS, sodium dodecyl sulfate; TM-4, tropomyosin (type)-4; UTR, untranslated region.

Grant sponsor: NIH; Grant numbers: HL-32184, HL-37702; Grant sponsor: American Heart Association (to LFL/DKD).

Robert W. Zajdel was supported by an American Heart Association postdoctoral fellowship for a portion of this work.

Belinda J. Spinner and Robert W. Zajdel share the First Authorship.

*Correspondence to: Dr. Dipak K. Dube, Department of Medicine, Upstate Medical University, 750 East Adams Street, Syracuse, New York 13210.
E-mail: DUBED@Upstate.edu

Received 5 October 2001; Accepted 13 February 2002
DOI 10.1002/jcb.10178

tion [Gunning et al., 1990; Schevzov et al., 1993].

Vertebrate tropomyosins (TMs) are a family of actin binding proteins encoded by a group of highly conserved genes that likely evolved as a result of gene duplication over the evolutionary period. There are four tropomyosin-encoding genes: α-TM, β-TM, hTMnm, and TM-4 [Lees-Miller and Helfman, 1991]. Each gene is known to encode a variety of isoforms via alternative splicing and/or the use of two promoters [Lin et al., 1985; Helfman et al., 1986; Wieczorek et al., 1988; Lees-Miller and Helfman, 1991]; the transcripts encode proteins of either 248 or 284 amino acids in length. The tropomyosins may also be divided into three categories: smoot muscle TMs, striated muscle TMs, and cytoplasmic TMs.

Striated muscle (cardiac and skeletal) isoforms in mammals are encoded by α- and β-TM genes. At the protein level, the striated muscle isoforms in heart are composed of alpha-/beta TM homo- or heterodimers, with the alpha/beta heterodimeric arrangement preferentially assembled [Brown and Schachat, 1985; Lehrer and Qian, 1990; Jancso and Graceffa, 1991]. The mammalian TM-4 gene is truncated and does not encode a striated muscle isoform. Rat TM-4 encodes only a single TM-4 isoform, which is a nonmuscle type [Lees-Miller et al., 1990]. The functional significance of the alpha-tropomyosin isoform has been explored in recent studies with transgenic mice [Blanchard et al., 1997]. However, the functional significance of TM-4 type tropomyosin to the organization and function of the heart has not been well studied.

Chicken striated muscle offers an example of different genes encoding tropomyosin isoforms in skeletal and cardiac muscle. Cardiac muscle TM in chicken [Forry-Schaudies et al., 1990; Fleenor et al., 1992] is encoded predominantly by a TM-4 type gene. The gene also encodes a nonmuscle isoform that is homologous with rat TM-4 and human TM30pl [MacLeod et al., 1987]. Amphibian heart also contains a tropomyosin isoform predominately encoded by a TM-4 gene. Two tropomyosin isoforms; a nonmuscle, low molecular weight isoform and a high molecular weight striated muscle isoform were found to be encoded by a TM-4 type gene in *Xenopus* adult heart [Hardy et al., 1995]. One of these isoforms, XTMCa encoded a polypeptide that was striated muscle size (284 amino acids) instead of the typical 248 amino acid nonmuscle TM-4 isoform. This XTMCa isoform had 97% aa (amino acid) homology with the chicken cardiac tropomyosin.

A cardiac mutation in an amphibian, Mexican axolotl (*Ambystoma mexicanum*), has reduced overall expression of tropomyosin in the ventricle. This mutation provided a unique tool to examine the expression of tropomyosin isoforms in embryonic hearts.

Three isoforms of tropomyosin have been identified in the axolotl, two putatively encoded by the alpha-gene, Axolotl Tropomyosin Cardiac-1 (ATmC-1 and ATmC-2) [Luque et al., 1994, 1997]. The third, characterized here as ATmC-3, is most likely a TM-4 type encoded by a separate gene. This isoform was demonstrated to be present in embryonic heart by RT-PCR and in situ hybridization; whereas in *Xenopus*, it was found to be in adult heart only. We also demonstrated a functional necessity of the TM-4 type tropomyosin for contraction in the embryonic vertebrate heart. Transfection of exon-specific antisense oligonucleotide (AS-ODN) into normal hearts disrupted the organization of the myofibrils and contractions. RT-PCR indicated a reduction in transcript levels, and specificity of the AS-ODN was confirmed by in vitro analysis of total RNA. Furthermore, ectopic expression of ATmC-3 in the ventricles of mutant hearts showed that the TM-4 type striated muscle isoform promoted the formation of organized myofibrils.

MATERIALS AND METHODS

Embryo Care

Normal and cardiac mutant axolotl embryos were obtained from matings between heterozygous (+/c × +/c) animals from the Indiana University axolotl colony and the axolotl colony at SUNY Upstate Medical University. Animals were maintained in aquaria in 50% Holfreter's solution (29 mM NaCl, 0.45 mM $CaCl_2$, 0.33 mM KCl, 0.1 mM $MgSO_4$, and 4.76 mM $NaHCO_3$) and fed commercial salmon pellets. The embryos were staged according to the standard stag-ing system [Bordzilovskaya et al., 1989].

Cloning and Sequencing of ATmC-3

The initial ATmC-3 clone, Heart2, which encompassed a portion of exon 9a and the entire 3′ untranslated region (UTR), was detected by cloning a 3′ Rapid Amplification of cDNA Ends (3′ RACE) product from total RNA of embryonic

hearts. Briefly, the 3′ RACE reaction was accomplished by first strand cDNA synthesis of approximately 1 μg total RNA using an oligo dT with an adapter primer tail. The cDNA was then amplified with a sense oligonucleotide and another adapter primer that was complementary to the one used for first strand synthesis. Subsequently, this clone was radiolabeled with [α^{32}P] dCTP in a PCR reaction and used to screen an axolotl juvenile heart cDNA library [Wieczorek et al., 1988]. The phage and host bacteria, *Escherichia coli* Y1090, were incubated together for 15 min at 37°C. Molten 0.75% LB agar was added and the mixture was plated on 1.5% LB agar plate at a concentration of 50,000 plaques per plate. Filter lifts were performed in duplicate the following morning on each plate using Schleicher and Schuell maximum strength Nytran Plus membranes. The first round of screening yielded positive clones which were plaque purified in two dilutions, then amplified with the polymerase chain reaction using λ3 sequence and λ5 sequence primers. The λ3/λ5 amplified PCR products of 6b (700 bp), 2b (900 bp), and 3b (800 bp) were cloned into the T/A cloning vector pCR 2.1 and six recombinants of each were randomly selected. The clones were grown in LB media in the presence of carbenicillin, dot blotted, and hybridized again to the internal detector oligonucleotide TmBS (−)2. The selected clones were isolated and sequenced at the Cornell University DNA Core Facility. The clones were of various lengths of the same sequence and included the sequence of the Heart2 clone. The longest of the three, approximately 900 bp, was clone Tm2b3. The strategy for cloning the ATmC-3 cDNA is outlined in Figure 1.

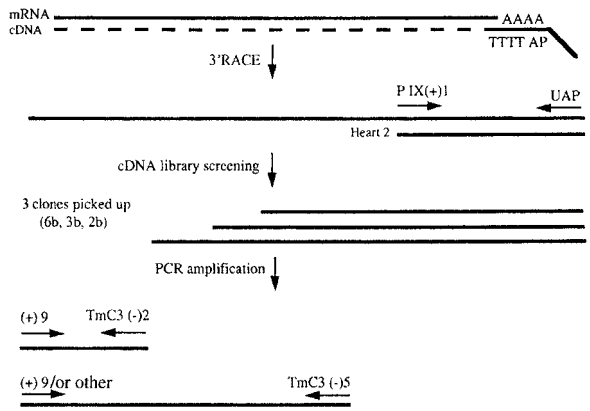

Fig. 1. Cloning strategy for ATmC-3 cDNA. The full-length ATmC-3 clone was derived from a combined PCR and library screening approach. Initially, a segment containing the putative exon 9 as well as the 3′ UTR was amplified using the 3′ RACE technique, and then the approximately 350 nt fragment was cloned. The juvenile axolotl cDNA library was then screened using this initial clone, named Heart2. Three clones of different sizes were isolated, all of which contained the 3′-UTR and various lengths of upstream sequence. The 3′ end of the coding sequence was obtained through PCR amplification, with subsequent cloning and sequencing, and then the overlap was verified by amplifying a larger length of DNA.

Total RNA Extraction

Embryos were washed four times in Steinberg's [Zackson and Steinberg, 1986] buffered salt solution (58 mM NaCl, 0.67 mM KCl, 0.9 mM $CaCl_2$, 0.2 mM $MgSO_4$, 4.6 mM HEPES, pH 7.4 containing 1% antibiotic/antimycotic at a final concentration of penicillin G sodium 100 U/ml, 0.1 g/ml streptomycin sulfate, 0.25 μg/ml amphotericin B (Gibco Life Technologies, Grand Island, NY). Prior to dissection, the embryos were anesthetized in MS-222 (tricaine methanesulfonate). Total RNA was extracted from the extirpated tissues using Ambion Totally RNA extraction kit. The total RNA was DNase treated with Gibco BRL RNase-free DNase for 15 min at room temperature, then phenol: chloroform extracted and precipitated with ethanol at −70°C for 1 h or overnight at −20°C. RNA purity and concentration were determined using a Pharmacia Biotech GeneQuant II RNA/DNA calculator.

Phylogenetic Analysis

The amino acid sequence of the axolotl ATmC-3 was deduced using the MAP and ExtractPeptide program of the UWGCG software package. The most homologous sequences from the GenBank were obtained using the TFASTA program. The extracted protein sequences were then aligned with the GAP alignment program [Needleman and Wunsch, 1970]. Subsequently, the phylogenetic analysis with the resulting matrix was completed by the Maximum Parsimony method using the PAUP 3.0 program [Swofford, 1991]. Bootstrap analysis, a computer-based technique for assessing the accuracy of almost any statistical estimate including phylogenetic trees, was carried out for 100 replication cycles [Swofford, 1991].

Northern Blot Analysis

Total RNA was extracted from Stage 41/42 heart of the axolotl embryo as described above. An estimated 10 μg of total RNA from each tissue type were processed for Northern blot

analysis following standard protocol [Sambrook et al., 1989].

Reverse Transcriptase Polymerase Chain Reaction

Reverse transcriptase polymerase chain reaction (RT-PCR) with RNA from embryonic and adult heart and skeletal muscle was performed to evaluate the expression of the ATm-C-3 using previously published protocol [Luque et al., 1997].

In Situ Hybridization

Stage 35 normal, Stage 38 and 41 normal, and mutant embryos were fixed for 2 h at room temperature with constant agitation in 1X MEMFA (0.1 M MOPS pH 7.4, 2 mM EGTA, 1 mM $MgSO_4$, 3.7% Formaldehyde), then paraffin embedded, sectioned at 8 μm and mounted on Fisher brand Superfrost Plus microscope slides. The probes were prepared digesting the DNA with either Hind III or Xho I restriction endonuclease for 3 h at 37°C, then phenol: chloroform extraction followed by ethanol precipitation at −70°C for 1 h or overnight. The in vitro transcription reaction was completed in a 20 μL total volume using 1 μg DNA in buffer (400 mM Tris-HCl, pH 8.0; 60 mM $MgCl_2$, 100 mM dithiotreitol (DTT), 20 mM spermidin) and 40 units of enzyme, T7 RNA polymerase for the Hind III digested DNA and SP6 RNA polymerase for the Xho I digested DNA. The RNA was treated with 1 unit RNase-free DNase (Gibco BRL) for 15 min at 37°C, followed again by phenol: chloroform extraction at −70°C for 1 h or overnight. The RNA concentration was estimated using a Pharmacia Biotech GenQuant II RNA/DNA calculator. Additionally, DIG incorporation was evaluated by electrophoresing the sample on a 1.5% agarose gel, then transferring overnight to GeneScreen nylon membrane in 50 mM NaOH; the color reaction was done using Genius kit buffers and B-M Purple AP Substrate (Boehringer-Mannheim) according to the manufacturer's protocol. The in situ procedure was adapted from the protocol of Vize et al., 1991, as previously described [Gaur et al., 1998].

Preparation of Exon-Specific Oligonucleotides

Sense (S-ODN) and anti-sense (AS-ODN) oligonucleotides were designed for exon 2 of the ATmC-3 tropomyosin isoform. The antisense ATmC-3 chimeric nucleotide was T*A*C* T*AG CTC GTC CTC AAG C*T*G*C* and for sense ^{f}G*C*A* GCT TGA GGA CGA GCT A*G*T *A; where *N represents a phosphorothioate blocked nucleotide and ^{f}G represents G tagged with fluorescein at the 5′ end (IDT, Inc.)

Preparation of the pSI.ATmC-3 Expression Constructs

ATmC-3 cDNA was amplified by PCR using 5′-TCGGAATTCCCGCTCCCT GACACCGGT−3′ (+ve) and 5′-GGGGAATTCCGATCACAT-CAGAGTGGA−3′ (−ve) primer-pair. We added an EcoR I site at the 5′ end of both positive and negative primers. The amplified products were digested with EcoR I and subsequently gel purified (Qiagen, Inc.) following the manufacturer's protocol. The digested DNA was then ligated to the EcoR I digested pSI vector (Promega) with T4 DNA ligase (Gibco BRL) and transfected into the competent *E. Coli* cells (Invitrogen). After colony hybridization, the positive clones were picked up and the DNA was prepared for DNA sequence analysis (Cornell University DNA sequence facility, Ithaca NY).

Cationic Liposome Mediated Transfection in Whole Hearts

Transfection of oligonucleotides and cDNA were performed according to previously published methods [Zajdel et al., 1998]. Transfected whole hearts were maintained in culture for 5 days.

Confocal Microscopy

Whole mount immunostaining and confocal microscopy were performed according to our published procedures [Zajdel et al., 1998]. Monoclonal tropomyosin antibody [CH1, Lin et al., 1985] or monoclonal alpha-actinin antibody (Sigma) were used for the immunodetection of proteins. Specimens were viewed on a BioRad MRC 1024ES confocal laser system mounted on a Nikon Eclipse E600 microscope. Control hearts and treated hearts were examined using identical confocal settings. A simultaneous or sequential (double staining) Z-series was made for each. Digital image processing was performed using Adobe Photoshop.

In Vitro Analysis of the Isoform Specificity for Sense and Antisense Oligonucleotides

Total RNA (5 μg) from axolotl heart was annealed with 10 pmoles of isoform specific

sense or anti-sense oligonucleotide at 65°C for 5 min, after which the annealed mixture was chilled on ice. One microliter of RNase inhibitor was added to the annealed mixture with 1 μL of RT-buffer, and 1 μL of RNase H (Clontech superscript First Strand Synthesis Kit). The mixture was incubated at 37°C for 20 min followed by denaturation at 70°C for 10 min to inactivate the enzyme. The 10 μL reaction was then chilled. RT reaction was performed using 5 μL of the above reaction mix in a total volume of 20 μL following Clontech's standard oligo dT protocol. Finally, PCR amplification was carried out with 2 μL of the RT product using isoform specific primer-pairs followed by the Southern blot analysis with [^{32}P]-labeled isoform specific detector oligonucleotides. Nucleotide sequences for ATmC-3 were mentioned previously. ATmC-2 and ATmC-1 nucleotide sequences used for this experiment were the following:

ATmC-2 sense, 5′-G*C*A*CACTGCTGACGA-GAAA*G*C*C*-3′;
ATmC-2 anti-sense, 5′-G*C*G*GCTTTCTCG-TCAGCAGTG*T*G*C-3′;
ATmC-1 sense, 5′-AGTACTCGGAGTCCTTG-A-3′,
ATmC-1 anti-sense, 5′-A*G*G*ACTCCGAGT-ACTTGTC*C*A*A-3′.

RESULTS

Cloning and Sequencing of ATmC-3 cDNA

The full-length coding region of ATmC-3 was cloned and sequenced including the 3′ untranslated region (3′UTR). The initial clone of the putative exon 9a and the complete 3′UTR were detected using a 3′ Rapid Amplification of cDNA Ends (3′ RACE) (Fig. 1). This radiolabeled clone was used for screening of the juvenile heart cDNA library, which resulted in a greater portion of the sequence being available. The 5′-most sequence was isolated using a PCR based strategy, amplifying a portion of the transcript beginning at the initiation codon, and having sufficient overlap with the known sequence to ensure reliability of the result. The ATmC-3 transcript encodes a 284 amino acid protein, with highest homology, 97% at the amino acid level and 82% at the nucleotide level, to *Xenopus laevis* TM-4 type cardiac tropomyosin (Table 1). The sequence homologies to the known axolotl tropomyosins, ATmC-1 and ATmC-2 are 77 and 73%, respectively, at the cDNA level; the amino acid sequences are 94 and 89% homologous (not shown). The ATmC-1 isoform in the axolotl represents a typical alpha-type striated muscle isoform. The high degree of homology of the amino acids is explained by the tremendous conservation of the protein across the evolutionary period. However, the great difference at the coding level is due to divergence at the wobble position. Additionally, the 3′UTR is far longer than the alpha-type transcripts in the axolotl. Initial cloning and sequencing were accomplished using a sense oligonucleotide that began at the initiation codon (ATG) and was 21 bases in length. The transcript sequenced was 852 nucleotides in length, with a 3′ UTR providing approximately 350 nucleotides. The initiation codon, ATG, was at position 1; the termination codon, TAA was at position 853; the polyadenylation signal, AATAAA, was at position 1205 (Fig. 2).

Phylogenetic Analysis

The deduced amino acid sequence of ATmC-3 was aligned and compared with the most homologous tropomyosin proteins obtained from databases in GenBank through FASTA and/or TFASTA program of GCG software. A cladogram was constructed using the maximum parsimony technique to delineate the evolutionary relationships among the tropomyosins from a variety of organisms (Fig. 3). The muscle specific alpha-tropomyosins from avian, mammalian, and amphibian species form distinct clusters; also alpha-tropomyosin from aquatic species, specifically Zebrafish and Salmon, form a separate clade. *Xenopus* TM-4 cardiac isoform, cardiac alpha-tropomyosin from brown trout, and axolotl cardiac isoform, ATmC-3, were clustered together. However, *Xenopus* (anuran amphibian) and brown trout (fish) cardiac tropomyosins were in the same clade whereas ATmC-3 (urodele amphibian) was in the outgroup, suggesting a diversity of ATmC-3 from *Xenopus* and brown trout counterparts.

Temporal and Spatial Expression of ATmC-3 in Normal and Mutant Axolotl

Northern blot analysis of total RNA indicates a transcript of approximately 1,250 bases in length in the embryonic cardiac tissue isolated from Stage 41/42 embryonic axolotls (Fig. 4)

RT-PCR analysis of early embryonic stages indicated that the onset of mRNA expression

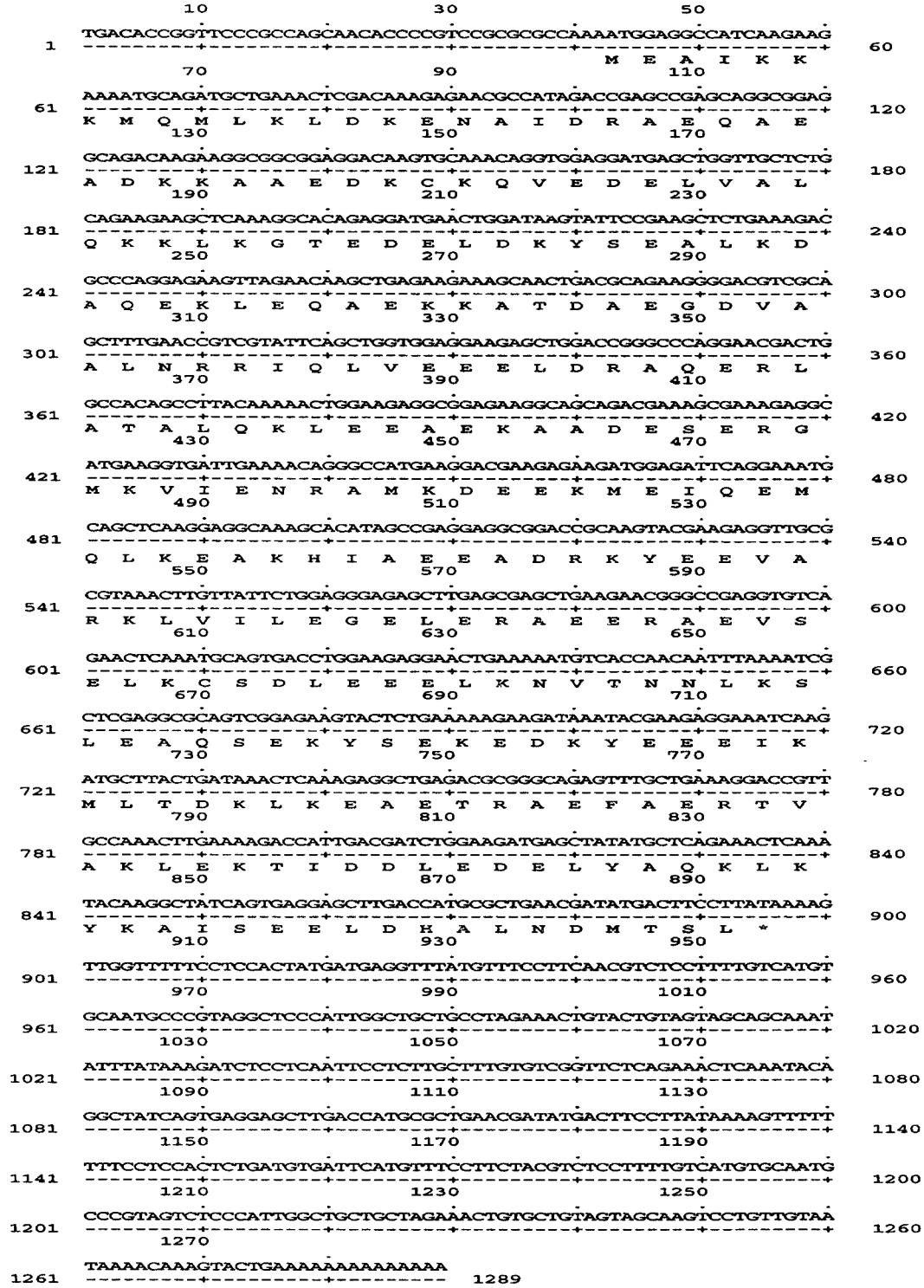

Fig. 2. ATmC-3 cDNA and deduced amino acid sequence. The open reading frame (ORF) starts from 43 nt and ends at 895 nt. *Denotes termination codon TAA. The coding region of ATmC-3 is 852 nt long that codes for 284 amino acids. **Line 1**: Numerical; **Line 2**: cDNA sequence; **Line 3**: Deduced amino acid sequence. Gene Bank Accession # AF480437.

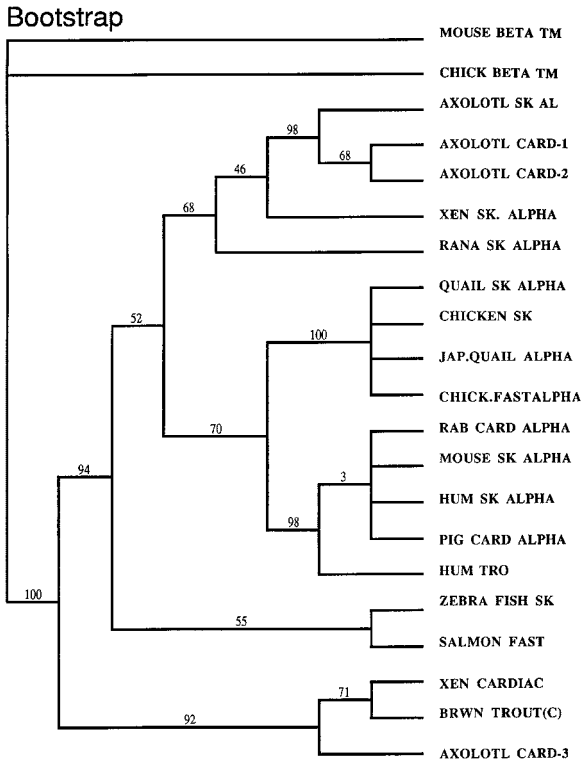

Fig. 3. Bootstrap analysis after 100 replications of the cladograms showing Phylogenetic relationship of ATmC-3 to various tropomyosins. The numbers on the branches show the percentages of the trees that support each branch. An accession number for each tropomyosin is as follows: Axolotl Cardiac-1: L35107; Axolotl Cardiac-2: U33449; Axolotl Cardiac-3: AF480437; Axolotl Sk. Muscle: L33450; Brown Trout: 266527; Chicken-beta: M64288; Chicken Fast alpha: M32441; Chicken Skeletal: J00910; Human Trop: M12125; Human Sk. Alpha: M19715; Japanese Quail: M15043; Mouse Beta: M81086; Mouse Sk. Alpha: X64831; Pig Cardiac Alpha: X66274; Quail Sk. Alpha: X04690; Rana Sk. Alpha: M24634; Rabbit Cardiac Alpha: V00892; Salmon Fast: L25609; Xenopus Sk. Muscle: X61273; Xenopus Cardiac: L35239; Zebra Fish Skeletal: M24635.

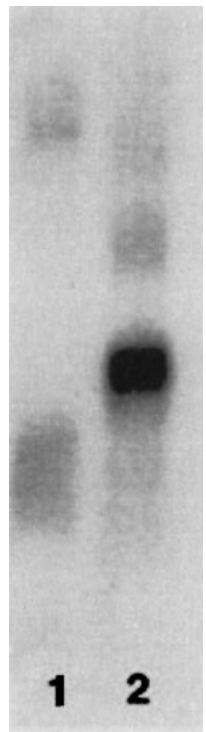

Fig. 4. Northern blot analysis for the expression of ATmC-3 transcript. **Panel A**: A 1.2% formaldehyde gel with an estimated 10 μg of total RNA from each tissue type. **Lane 1**: RNA ladder; **Lane 2**: Stage 41 embryonic heart total RNA. An α-^{32}P labeled probe corresponding to the putative exon 9 region including the 3′ untranslated region (UTR) was used to detect the message. The ATmC-3 transcript was approximately 1.25 kb in length.

begins beyond Stage 30, the latest pre-heartbeat stage typically evaluated (Fig. 5). In the early embryo, Stage 6, 10, 15, 20, 25, and 30 were evaluated. Expression of an alpha-type striated muscle isoform, ATmC-1 begins in the axolotl around Stage 10. The differing onset times for expression of the isoforms suggest a carefully orchestrated pattern of gene expression. The delayed onset of expression of ATmC-3 corroborates the Northern blot data suggesting that the isoform is cardiac specific. Additionally, the different pattern from the alpha-type transcript shows that the detection system used in both the Northern blot and RT-PCR is specific for this TM-4 isoform and does not have any overlapping detection of the highly similar alpha-type transcript. RT-PCR data with total heart RNA showed that ATmC-3 is expressed in adult hearts (results not shown).

RT-PCR experiments were also performed with total RNA isolated from heart and skeletal muscles of normal and mutant embryos at Stage 38 and 41 (Fig. 5). The results indicated ATmC-3 to be expressed predominantly in cardiac tissue at both stages, and interestingly, expressed in both the normal and mutant tissue. It has previously been demonstrated that the mutant hearts lacked tropomyosin protein [Starr et al., 1989]; however, it is evident that at least one tropomyosin isoform mRNA is present.

In situ hybridization was performed on paraffin sections of Stage 35 normal, Stage 38 and 41 normal, and mutant embryonic axolotls (Fig. 6). Staining results demonstrated the cardiac-specific expression of the transcript in both normal and the mutant embryos. Additionally, the relatively similar staining between the normal and mutant embryos confirmed that

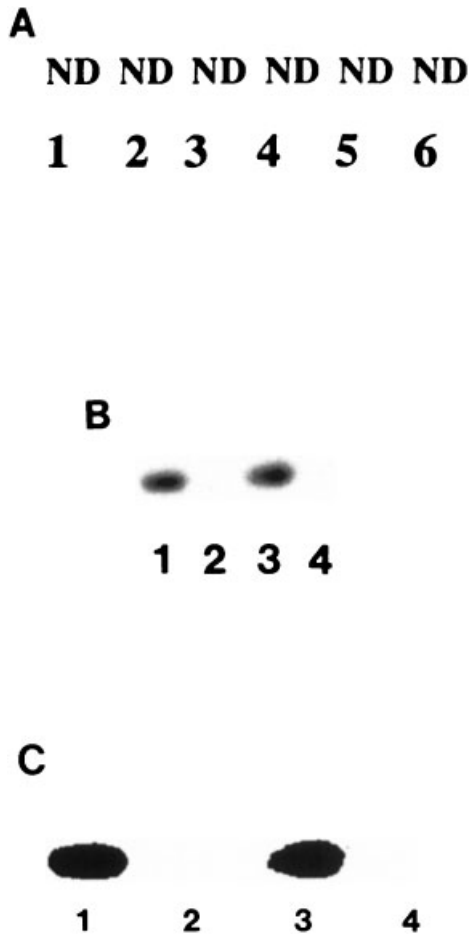

Fig. 5. RT-PCR analysis for evaluating the expression of ATmC-3 transcript at various stages of development and also in normal and mutant embryonic hearts. **Panel A**: **Lane 1**—Stage 6 whole embryo total RNA; **Lane 2**—Stage 10 whole embryo; **Lane 3**—Stage 15 whole embryo total RNA; **Lane 4**—Stage 20 whole embryo RNA; **Lane 5**—Stage 25 whole embryo total RNA; **Lane 6**—Stage 30 whole embryo RNA. ND, not detected. **Panel B**: **Lane 1**—Stage 38 normal heart total RNA; **Lane 2**—Stage 38 normal skeletal muscle total RNA; **Lane 3**—Stage 38 mutant heart total RNA; **Lane 4**—Stage 38 mutant skeletal muscle total RNA. **Panel C**: **Lane 1**—Stage 41 normal heart total RNA; **Lane 3**—Stage 41 normal skeletal muscle total RNA; **Lane 3**—Stage 41 mutant heart total RNA; **Lane 4**—Stage 41 mutant skeletal muscle total RNA. The PCR amplification was accomplished with primer-pair PIX (+) 1A/TmBS 1(−); the subsequent hybridization was with detector oligonucleotide TmBS 2(−) in all lanes.

the presence of the ATmC-3 transcript in the mutant heart was not an artifact due to amplification.

Disruption of Organized Myofibrils and Contractions by ATmC-3 Antisense Oligonucleotides

Inhibition of ATmC-3 expression with antisense oligonucleotide transfection resulted in a disruption of the organization of the myofibrils. Confocal microscopic analysis of normal control hearts stained with CH1 tropomyosin antibody demonstrates organized myofibrils throughout the sections and in all of the cells (results not shown). Transfection of normal hearts with ATmC-3 exon 2 specific sense chimeric oligonucleotide [5′-^{f}G*C*A* GCT TGA GGC GAG CTA* G*T*A*-3′] did not significantly alter the organization of the myofibrils (Fig. 7A). These FS-ODN transfected normal hearts retained their ability to contract with 8/8 still contracting during the 5 days preceding fixation. The sense oligonucleotide was tagged at the 5′ end with fluorescein so that entry of the sense oligonucleotide into the cardiac cells could be confirmed. After 2 days of transfection, green fluorescence was observed within the hearts (data not shown). Significantly, at 5 days of transfection all of the treated hearts had fluorescein within a majority of the cells, primarily in the nuclear areas (Fig. 7C). Cationic liposomes have been shown to deliver F-ODN to the nucleus while leaving the lipid in the cytoplasm [Zelphati and Szoka, 1996]. FS-ODN entered the whole hearts during transfection with localization to the nucleus without inhibiting the biosynthesis of ATmC-3 protein and with little disruption of the myofibril organization.

Organized myofibrils were significantly disrupted in normal hearts transfected with ATmC-3 exon 2 specific anti-sense oligonucleotide (AS-ODN) (Fig. 7B). Organized myofibrils were almost completely disrupted in the ventricles of some hearts, whereas regional disruption was observed in other hearts. Contractions stopped completely in 6 of the 10 of the AS-ODN transfected hearts. The average beats per minute in the remaining hearts (7.2 beats/min) was slower than FS-ODN transfected hearts (14 beats/min)

RT-PCR analysis was also performed with RNA from control normal hearts, normal hearts transfected with S-ODN, and normal hearts transfected with AS-ODN. Total cellular RNA was isolated from 50 hearts of each control group after 5 days of transfection. RT-PCR was carried out using ATmC-3 specific primer pair following published protocol [Gaur et al., 1995, 1998]. The results showed that the concentration of ATmC-3 transcript in control and sense oligonucleotide treated hearts were comparable (Fig. 8A). However, we did not detect the ATmC-3 transcript in AS-ODN treated hearts.

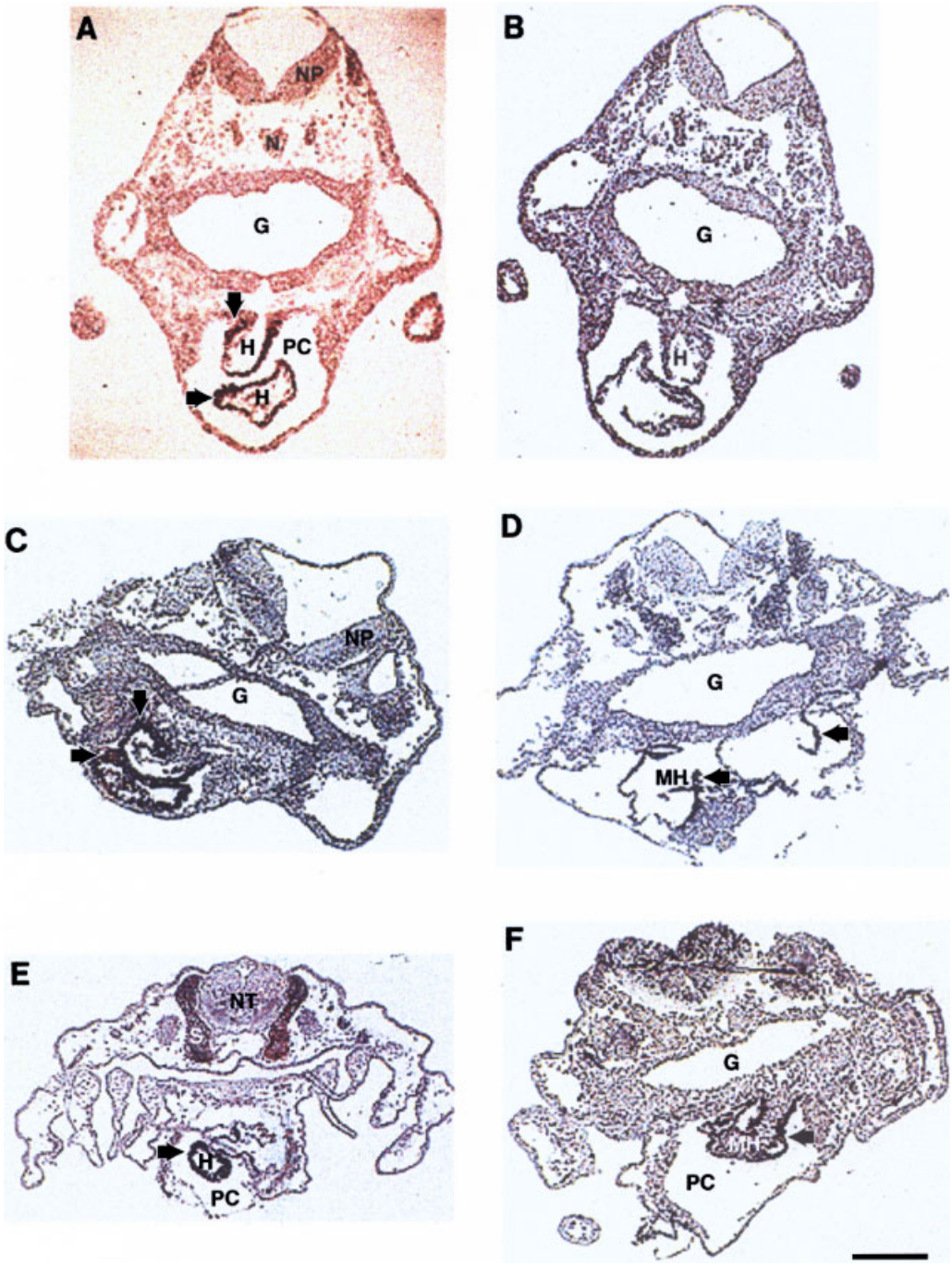

Fig. 6. In situ hybridization analysis for expression of ATmC-3 transcript in normal and mutant axolotl hearts. **Panel A**: Stage 35 axolotl embryo with antisense RNA probe (arrowheads highlight areas of positive staining). **Panel B**: Stage 35 axolotl embryo with sense RNA probe. **Panel C**: Stage 38 normal axolotl embryo with antisense RNA probe. **Panel D**: Stage 38 mutant axolotl embryo with antisense RNA probe. Mutant hearts begin to have morphological changes from this stage onward. **Panel E**: Stage 41 normal axolotl embryo with antisense RNA probe. **Panel F**: Stage 41 mutant axolotl embryo with antisense RNA probe. The probe was an approximately 350 base sequence of synthetic DIG labeled RNA encompassing the putative exon 9 and the 3′ untranslated region of the ATmC-3 sequence. (G-gut, H-heart, MH-mutant heart, N-notochord, NP-neural plate, NT-neural tube, PC-pericardial cavity, S-somite). Bar, 200 μm. [Color figure can be viewed in the online issue, which is available at www.interscience.wiley.com.]

Increased exposure of the X-ray film displayed a weak ATmC-3 signal. The amount of ATmC-3 transcript was quantified by densitometry and the NIH image program. These results showed the concentration of the ATmC-3 transcript was drastically reduced in AS-ODN transfected hearts but not in the FS-ODN hearts. This was most likely due to the action of the RNase H enzyme on the AS-ODN hybrid with the ATmC-3 transcript. ATmC-2 transcript was not reduced in the ATmC-3 AS-ODN transfected hearts indicating the specificity of the AS-ODN to ATmC-3. Thus, the action of the ATmC-3 AS-ODN was specific in reducing the level of the ATmC-3 transcripts in normal hearts.

The specificity of these oligonucleotides was also determined in vitro. Isoform specific S-ODN or AS-ODN was annealed with total RNA from embryonic axolotl hearts, the reaction products were treated with RNase H. RT-PCR was then performed with a gene specific primer pair followed by Southern blot analysis. Figure 8C demonstrates that annealing total RNA with ATmC-3 AS-ODN affected the concentration of ATmC-3 transcript only and not ATmC-1 or ATmC-2 transcript. ATmC-3 sense oligonucleotide did not affect either ATmC-3, ATmC-2, or ATmC-1 transcripts. The data demonstrated the specificity of the S-ODN and AS-ODN for in vitro and for the in vivo experiments. Therefore, transfection of exon 2 specific AS-ODN for ATmC-3 conclusively altered transcripts, protein expression, organization, and contractions in the ventricles of normal whole hearts.

Ectopic Expression of pSI.ATmC-3 Into Mutant Whole Hearts

Mutant axolotl hearts have greatly reduced levels of tropomyosin in the ventricles. This reduction contributes to few, if any organized myofibrils, and no contractions. Since the ventricles of the mutant hearts lack tropomyosin, we transfected ATmC-3 cDNA into mutant

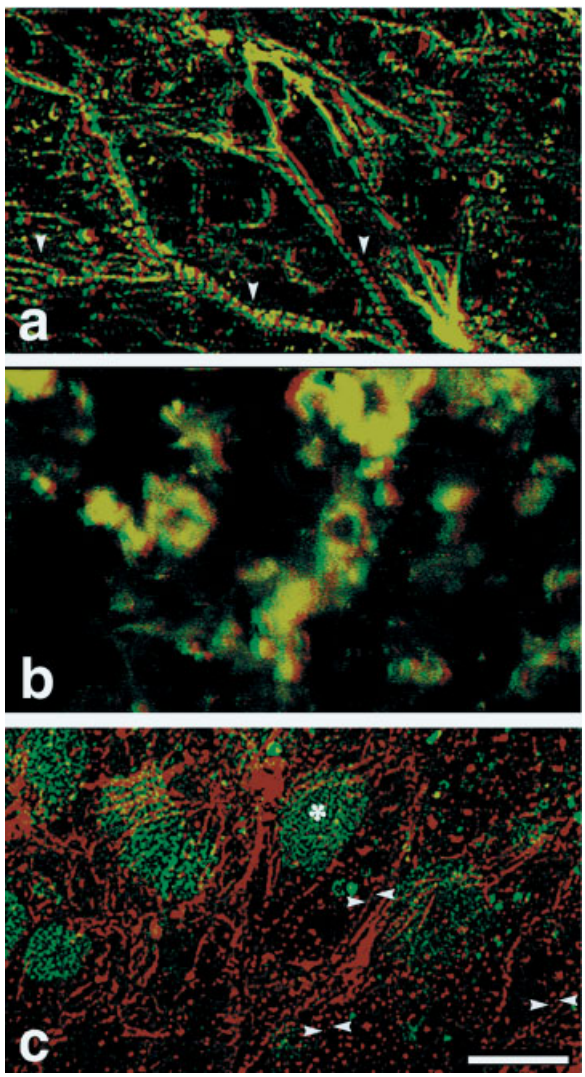

Fig. 7. Transfection of ATmC-3 specific sense and anti-sense oligonucleotides in whole hearts. **A**: Stereo anaglyph of a 24 section confocal laser scanning microscope z-series. The red and green colors are created by the confocal software and an offset is created. This type of image is shown because it demonstrates branching myofibrils in whole hearts. Periodic myofibril staining (CH1 tropomyosin antibody) was seen in ATmC-3 sense transfected normal whole hearts (arrowheads). Red/green glasses may also be used to visualize the myofibrils in pseudo three dimensions. **B**: Stereo anaglyph of normal heart transfected with ATmC-3 exon 2 specific anti-sense chimeric oligonucleotide, 5′-T*A*C*T*AGCTCGTCCTCAAGC*T*G*C*-3′, where *N represents the phosphothioate blocked oligonucleotide (IDT, Inc.). Myofibril organization was disrupted in a majority of the cardiomyocytes. Most of the tropomyosin appears to be in amorphous areas when expressed. Some of the cells do not appear to have a detectable level of tropomyosin. Gross morphology was normal and the cells appeared to be intact although myofibril structure was largely disrupted. **C**: Normal heart transfected with ATmC-3 exon 2 specific sense chimeric oligonucleotide, 5′-^{f}G*C*A*GCTTGAAGGCGAGC-TA*G*T*A*-3′, where *N represents phosphothioate blocked nucleotide and ^{f}G represents G tagged with Fluorescein at the 5′ end (IDT, Inc.). This image is a compressed z-series of two sections that was not stereo offset but used to demonstrate double staining. Isolated pieces of myofibrils that were contained within these sections of the cardiac cells were stained with tropomyosin antibody (red, arrowheads). This image is primarily useful for demonstrating the presence of green fluorescence (GFP) within the nuclear area of the cardiomyocytes by 5 days (asterisk). Bar, 20 μm.

hearts. Previously, we have shown that ectopic introduction of a mouse tropomyosin cDNA could promote myofibril formation in mutant hearts [Zajdel et al., 1998]. Mutant hearts transfected with axolotl ATmC-3 cDNA exhibited increased expression of tropomyosin protein and organized myofibrils in the ventricles (Fig. 9). Control mutant hearts lacked organized myofibrils in the ventricles.

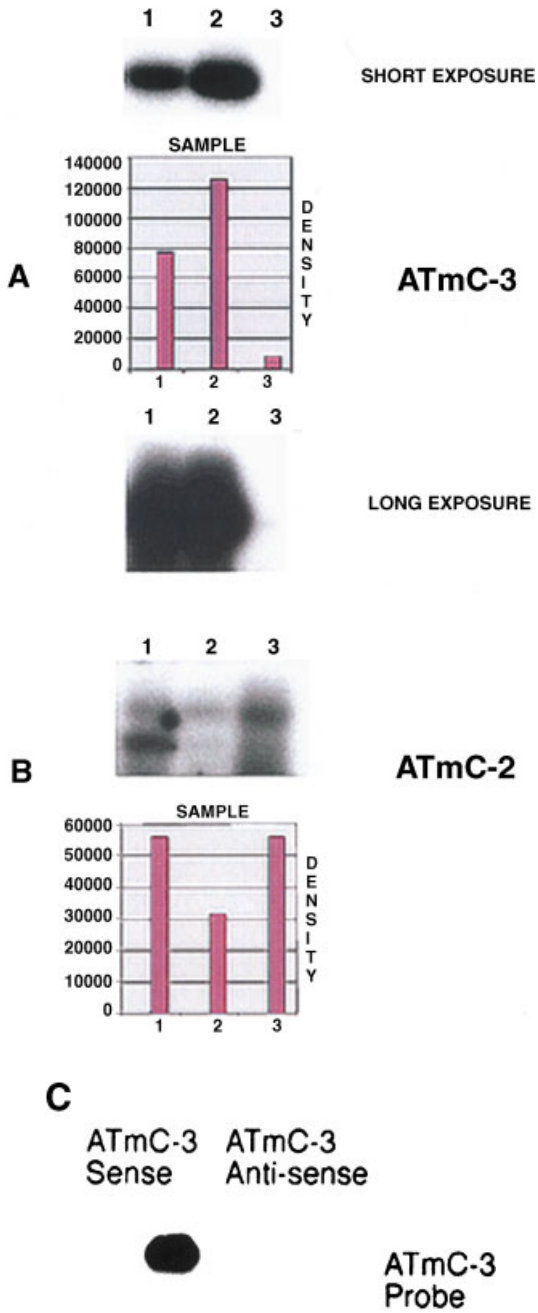

Fig. 8. Determination of relative concentration of ATmC-3 transcripts by RT-PCR in sense and anti-sense oligonucleotide transfected axolotl hearts; in vitro analysis of the specificity of the transfected oligonucleotides. **Panel A**: Total RNA was isolated from axolotl hearts transfected with ATmC-3 specific sense and anti-sense oligonucleotides (as in Fig. 7). RT-PCR and subsequent hybridization was carried out with ATmC-3 specific primer-pair and detector oligonucleotide respectively as stated under Materials and Methods. The autoradiograph was developed at 4 (upper panel for short exposure) and 24 h (bottom panel for long exposure). Densitometry scan was performed using NIH Image Program. The results showed drastic reductions in ATmC-3 transcripts in hearts transfected with ATmC-3 anti-sense oligonucleotides compared to that in sense oligonucleotide transfected hearts. **Lane 1**: RNA from control hearts. **Lane 2**: RNA from sense oligonucleotide transfected hearts. **Lane 3**: RNA from ATmC-3 specific anti-sense oligonucleotide transfected hearts. **Panel B**: Determination of the concentration of ATmC-2 transcript in control and ATmC-3 specific anti-sense oligonucleotide transfected hearts. RT-PCR was carried out to determine the concentration of ATmC-2 in transfected hearts. ATmC-2 specific primer-pair [5′-ATGGACGCCATCAAGAA-GAAG-3′ (+ve)/ 5′-TTACATTGAAGTCATATCGTTGAG-3′ (−ve) and detector oligonucleotide (5′- AGGGTGCTGGAT-GAACTGCACAA-3′) were used for the amplification of ATmC-2 transcripts as described earlier [Luque et al., 1997]. The results show that the transfection of either ATmC-3 specific sense or anti-sense oligonucleotides did not affect the concentration of ATmC-2 in axolotl hearts. **Lane 1**: RNA from control hearts; **Lane 2**: RNA from ATmC-3 specific sense oligonucleotide transfected hearts; **Lane 3**: RNA from ATmC-3 specific anti-sense oligonucleotide transfected hearts. The results from Figures 8A and B suggest that hearts transfected with ATmC-3 specific anti-sense oligonucleotide specifically lowers the concentration of ATmC-3 transcript but not of ATmC-2. ATmC-3 specific sense oligonucleotide does not affect the concentration of ATmC-3 transcripts. **C**: Determination of the specificity of the sense and anti-sense oligonucleotides used in vivo by in vitro experiments using RNase H and RT-PCR. In this experiment, total RNA isolated from axolotl heart was annealed with sense or anti-sense oligonucleotides and the annealed reaction mixture was digested with RNase H (Gibco BRL). Finally RT-PCR was carried out with the RNase H treated RNA using our standard protocol as described under Materials and Methods. Southern blot analysis was performed with ATmC-3 specific detector oligonucleotide [Luque et al., 1997]. The results show that the ATmC-3 transcript was not reduced with sense oligonucleotide (first lane) whereas the anti-sense oligonucleotide significantly reduced the amount of ATmC-3 transcripts due to RNase H treatment. This shows the specificity of the sense and anti-sense oligonucleotides used for transfection in vivo. **ATmC-3 sense lane**: RNA was annealed with sense oligonucleotide specific for ATmC-3 and subsequent RT-PCR was carried out with ATmC-3 specific primer-pairs and detector oligonucleotides. **ATmC-3 anti-sense lane**: RNA was annealed with ATmC-3-specific anti-sense oligonucleotides in vitro. RT-PCR was carried out with ATmC-3 specific primer-pairs and detector oligonucleotides. The results show that annealing of anti-sense oligonucleotides but not the sense counter part allows degradation of ATmC-3 transcripts by RNase H. The results also show the specificity of the sense and anti-sense oligonucleotides of ATmC-3 that have been used for in vivo experiments (A and B). [Color figure can be viewed in the online issue, which is available at www.interscience.wiley.com.]

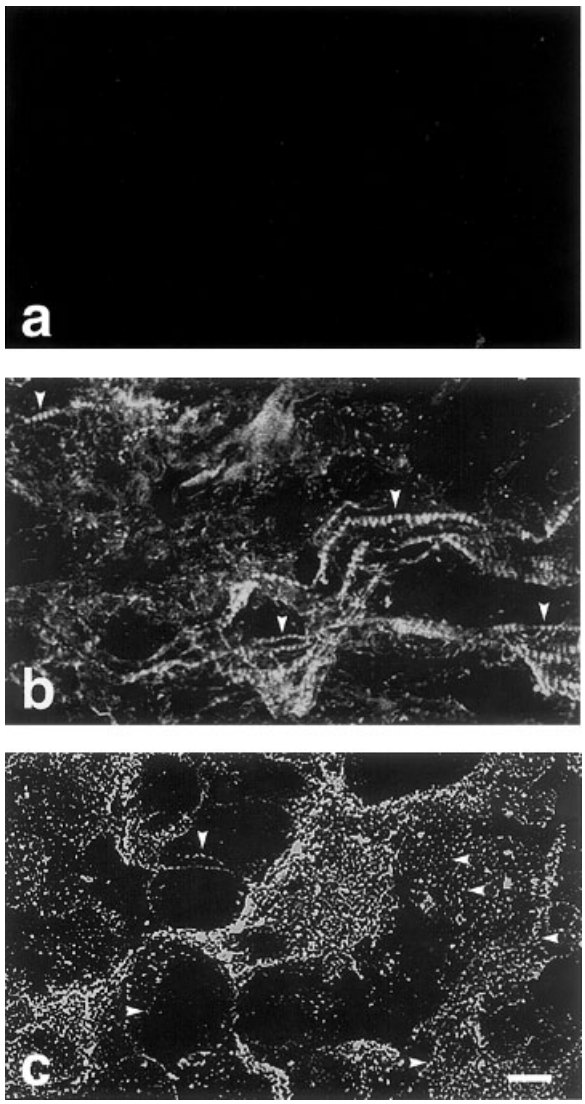

Fig. 9. Transfection of whole mutant hearts with pSI ATmC-3 cDNA. **A**: Compressed z-series of a control mutant heart stained with CH1 anti-tropomyosin antibody. The mutant ventricle has greatly reduced expression of the protein detected by CH1. Identical confocal parameters were used on this control heart as the experimental hearts. **B**: Compressed z-series of a mutant heart transfected with pSI ATmC-3 cDNA, treated for 48 h and cultured for a total of 5 days. Tropomyosin staining was clearly increased compared to the mutant control. Small and larger sarcomeric myofibrils have formed in many of these cardiomyocytes (arrowheads). **C**: Compressed z-series of a mutant heart transfected with pSI ATmC-3 cDNA and stained for alpha-actinin. Sarcomeric myofibrils branching in many directions can be seen in specific areas of the cardiomyocytes (arrowheads). Bar, 10 μm.

DISCUSSION

The assembly and maintenance of the sarcomere is dependent on regulated gene expression of specific contractile proteins or isoforms [Epstein and Fischman, 1991; Ordahl, 1992]. Diversity of tropomyosin isoforms occurs in different tissues or cells by alternative splicing and differential gene expression [Wieczorek et al., 1988; Goodwin et al., 1991; Hardy et al., 1991; Fleenor et al., 1992; Pittenger et al., 1994; Lin et al., 1997]. Knowledge of the number of isoforms is expanding but information on the importance of these isoforms to the specific functions of the individual cells is largely unknown. In general, tropomyosin muscle isoforms are important in muscle contraction, especially regarding interaction with actin and troponin [Smillie, 1979; Zot and Potter, 1987] and nonmuscle tropomyosin isoforms have been found to be important to the formation of the cytoskeleton [Pittenger et al., 1994]. Reduced expression of tropomyosin may also be involved in cancerous transformations [Prasad et al., 1993; Boyd et al., 1995].

Regulation of the expression of specific TM isoforms within a cell is also relatively unknown but likely related to a cell's specific function. Earlier studies have proposed that differential control of tropomyosin mRNA levels during myogenesis can occur as a result of an isoform competition-auto regulatory compensation mechanism [Gunning et al., 1990]. Similarly, actin isoforms, γ and β, were found to be differentially regulated at the level of mRNA accumulation. This regulation of actin isoforms may be intimately associated with the interaction of a specific tropomyosin isoform. Specifically, nonmuscle tropomyosins (248 aa) were more closely regulated with the nonmuscle actins [Gunning et al., 1990]. More recent studies have hypothesized the translational control of mRNA expression and regulation of tropomyosin proteins [Pieples and Wieczorek, 2000].

Three isoforms of axolotl tropomyosin have been isolated, sequenced, and designated ATmC-1, ATmC-2, and ATmC-3 [Luque et al., 1994; Luque et al., 1997]. We believe that two (ATmC-1 and ATmC-2) are encoded by the putative alpha-TM gene and the third (ATmC-3) is encoded by a TM-4 type gene. Northern blot analysis and RT-PCR of ATmC-3 showed expression predominantly in heart with very little in skeletal muscle. Two embryonic stages were examined and detection in these stages confirmed the specificity of ATmC-3 to the heart.

We have also cloned and sequenced the ATmC-3 cDNA from mutant axolotl hearts that

lack tropomyosin in the ventricle. However, we have not detected any mutations either in the 5′UTR or in the coding region of the ATmC-3 transcript (data not shown). The results strongly suggest that the tropomyosin deficiency in the mutant is not due to the formation of a premature codon in the ATmC-3 gene. Rather, the deficiency of tropomyosin protein is most likely due to an insufficiency at a post-transcriptional level. This could be due to a mutation at the 3′-UTR, which makes the ATmC-3 transcript, thereby altering translation in the mutant hearts. Alternatively, an inhibitory protein that may be overexpressed in the mutant hearts may specifically bind with the ATmC-3 transcripts. This complex may prevent the translation of the ATmC-3 transcript.

The lack of organized myofibrils in mutant hearts has been confirmed by ultrastructural and immunohistochemical methods [Lemanski, 1973]. Biochemical, immunohistochemical, and radioimmunoassay also indicated that the tropomyosin levels were significantly reduced [Moore and Lemanski, 1982, Starr et al., 1989]. The effect of the tropomyosin deficiency was further substantiated in the mutant heart by the findings that ectopic expression of murine alpha-tropomyosin cDNA or lipofection of purified rabbit TM protein could result in the formation of organized myofibrils [Zajdel et al., 1998]. RNA from normal axolotl heart has been shown to increase tropomyosin levels and promote myofibril formation in mutant hearts [Davis and Lemanski, 1987; Lemanski et al., 1996]. The regulatory mechanism used to promote or inhibit the translation of a specific tropomyosin is unknown.

In the current experiments, we transfected a specific axolotl tropomyosin cDNA into mutant hearts and organized myofibrils also formed. Thus, the ATmC-3 TM-4 type tropomyosin can replace missing tropomyosin in mutant hearts. In combination with the AS-ODN experiments, this suggests that the missing tropomyosin may be ATmC-3. It also supports the hypothesis that a 284 aa striated muscle TM-4 type tropomyosin can form organized myofibrils similar to alpha-tropomyosin. Therefore, axolotl heart contains a TM-4 type tropomyosin that can function similar to chicken TM-4. However, we found expression of ATmC-3 in both adult and embryonic heart, whereas TM-4 type expression in *Xenopus* was only found in adult heart [Hardy et al., 1995].

Our data support Hardy's earlier results regarding the evolutionary relationship of the co-expression of the TM-4 gene and an alpha-type TM in amphibians [Hardy et al., 1995]. Through the course of vertebrate evolution, it is evident that the co-expression was lost, leaving avians with cardiac expression of exclusively TM-4 and mammals with expression of alpha and/or beta tropomyosin. It appears that advanced vertebrates do not co-express a TM-4 cardiac transcript and an alpha- or beta-tropomyosin gene. Hence, one may assume that the need for the TM-4 protein was lost along the evolutionary path.

The functional significance of TM-4 type tropomyosin in the heart was examined by transfection of ATmC-3 exon specific antisense oligonucleotides and ATmC-3 cDNA. Expression of the ATmC-3 transcript was effectively blocked with the anti-sense oligonucleotide and the expression of ATmC-1 (results not shown) or ATmC-2 transcripts were not affected. In vitro analysis of the specificity of the ATmC-3 antisense oligonucleotide demonstrated the expected specific action. Therefore, we believe these various experiments clearly show that the ATmC-3 transcript level was reduced and not the other tropomyosins. Concomitantly, myofibril organization was disrupted and less tropomyosin protein was localized with the CH1 antibody. Finally, contractions were stopped in some of the hearts transfected with AS-ODN. Blocking the expression of TM-4 tropomyosin altered the formation of organized myofibrils in the ventricles of the normal hearts.

Further examination of the regulation of the specific tropomyosin isoforms and their significance within specific cells may help determine the regulatory pathways involved with myofibril formation and maintenance. In this study, we show that a TM-4 type tropomyosin was found in embryonic and adult heart of an amphibian, in contrast to *Xenopus*, which had TM-4 expression only in adult heart. Transfection of isoform specific oligonucleotides altered the expression of this isoform and organization of myofibrils. Interestingly, we did not find a decrease in the ATmC-3 transcript in untreated mutant hearts. Although, blocking the expression ATmC-3 expression alters myofibril organization and reduces tropomyosin staining, further study will be needed to determine if the expression of ATmC-3 in mutant hearts is

TABLE I. ATmC-3 cDNA and Deduced Amino Acid Sequence Homology

Accession number	Species name	cDNA (%)	AA (%)
L35239	*X. laevis* cardiac (TM-4)	82	97
L61273	*X. laevi* α skeletal TM	79	95
Z66527	*S. trutta* cardiac TM	79	94
M24634	*R. temporaria* α skeletal TM	78	96
M17914	Japanese quail α TM	79	94
S78854	Rabbit α skeletal TM	78	94
X64831	*M. musculus* skeletal TM	78	94
X66274	*S. scrofa* cardiac α TM	78	93
M36337	Chicken α TM (clone ctm 7)	78	94
M19713	Human α skeletal TM	77	94
L35107	*A. mexicanum* ATmC-1	77	94
U33449	*A. mexicanum* ATmC-2	73	89
M97554	*B. glabrata* (snail)	61	71

Sequences were analyzed with BESTFIT and TFASTA programs of the GCG software program. The first column lists the accession numbers sequences in the database. The species abbreviations are as follows: *A. Mexicanum*, Mexican axolotl; *X. laevis*, African clawed frog; *R. temporaria*, frog; *S. Salar*, trout; *M. musculus*, house mouse; *D. Rerio*, Zebrafish; *S. Scrofa*, pig; *B. glabrata*, snail. The third column lists the percent homology between the cDNA sequences. The fourth column lists the percent homology between the deduced amino acid sequences.

lower due to inhibition of synthesis at the translational level.

ACKNOWLEDGMENTS

The authors thank D. Packard, D. Robertson, and T. Poole for critical comments. The CH1 antibody was obtained from the Developmental Hybridoma Bank maintained by the Department of Pharmacology and Molecular Sciences, Johns Hopkins University, School of Medicine, Baltimore MD, and the Department of Biology, University of Iowa, Iowa City, IA, under contract NO-1HD-6-2915 from the NICHD. This work was supported by NIH grants HL-32184 and HL-37702 and a Grant-in-aid from the American Heart Association to LFL/DKD. RWZ was supported by an American Heart Association postdoctoral fellowship for a portion of this work.

REFERENCES

Blanchard EM, Iizuka K, Christe M, Conner DA, Geisterfer-Lowrance A, Schoen FJ, Maughan DW, Seidman CE, Seidman JG. 1997. Targeted ablation of the murine alpha-tropomyosin gene. Circ Res 81:1005–1010.

Bordzilovskaya NP, Detlaff TA, Duhon ST, Malacinski GM. 1989. Developmental Stage series of axolotl embryos. In: Armstrong JB, Malacinski GM, editors. Developmental biology of the axolotl. New York: Oxford University Press. p 210–291.

Boyd J, Risinger JI, Wiseman RW, Merrick BA, Selkirk JK, Barrett JC. 1995. Regulation of microfilament organization and anchorage-independent growth by tropomyosin I. Proc Natl Acad Sci USA 92:11534–11538.

Brown HR, Schachat FH. 1985. Renaturation of skeletal muscle tropomyosin: implication for in vivo assembly. Proc Natl Acad Sci USA 82:2359–2363.

Cho Y-J, Hitchcock-DeGregori SE. 1991. Relationship between alternatively spliced exons and functional domains in tropomyosin. Proc Natl Acad Sci USA 88:10153–10157.

Davis L, Lemanski LF. 1987. Induction of myofibrillogenesis in cardiac lethal mutant axolotl hearts rescued by RNA derived from normal endoderm. Development 99: 145–154.

Epstein HF, Fischman DA. 1991. Molecular analysis of protein assembly in muscle development. Science 251: 1039–1044.

Fleenor DE, Hickman KH, Lindquester GJ, Devlin RB. 1992. Avian cardiac tropomyosin gene produces tissue-specific isoforms through alternative RNA splicing. J Muscle Res Cell Motil 13:55–63.

Forry-Schaudies S, Maihle NJ, Hughes SH. 1990. Generation of skeletal, smooth, and low molecular weight non-muscle tropomyosin isoforms for the chicken tropomyosin 1 gene. J Mol Biol 211:321–330.

Gaur A, Lemanski LF, Dube DK. 1995. Identification and expression of a homologue of the murine *Hox*A5 gene in the Mexican axolotl (*Ambystoma mexicanum*). Gene 162:249–253.

Gaur A, Bhatia R, Spring-Mills E, Lemanski LF, Dube DK. 1998. The heart of metamorphosing Mexican axolotl but not that of the cardiac mutant is associated with up-regulation of *Hox*A5. Biochem Biophys Res Commun 245: 746–751.

Goodwin LO, Lees-Miller JP, Leonard MA, Cheley SB, Helfman DM. 1991. Four rat fibroblasts tropomyosin isoforms are expressed via alternative RNA splicing and the use of two promoters. J Biol Chem 266:8408–8415.

Gunning P, Gordon M, Wade R, Gahlmann R, Lin C-S, Hardeman E. 1990. Differential control of tropomyosin mRNA levels during myogenesis suggests the existence of an isoform competition-autoregulatory compensation control mechanism. Dev Biol 138:443–453.

Hardy S, Fiszman MY, Osborne HB, Thiebaud P. 1991. Characterization of muscle and nonmuscle *Xenopus laevis* tropomyosin mRNAs transcribed from the same gene. Eur J Biochem 202:431–440.

Hardy S, Theze N, Lepetit M, Allo M, Thiebaud P. 1995. The *Xenopus laevis* TM-4 gene encodes non-muscle and cardiac tropomyosin isoforms through alternative splicing. Gene 156:265–270.

Helfman DM, Cheley S, Kuismanen E, Finn LA, Yamawaki-Kataoka Y. 1986. Nonmuscle and muscle tropomyosin isoforms are expressed from a single gene by alternative RNA splicing and polyadenylation. Mol Cell Biol 6:3582–3595.

Jancso A, Graceffa P. 1991. Smooth muscle tropomyosin coiled-coil dimmers. Subunit composition, assembly, and end-to-end interaction. J Biol Chem 266:5891–5897.

Lees-Miller JP, Helfman DM. 1991. The molecular basis of tropomyosin diversity. Bioessays 13:429–437.

Lees-Miller JP, Yan A, Helfman DM. 1990. Structure and complete nucleotide sequence of the gene encoding rat fibroblast tropomyosin 4. J Mol Biol 213:399–405.

Lehrer SS, Qian Y. 1990. Unfolding/refolding studies of smooth muscle tropomyosin. Evidence for a chain exchange mechanism in the preferential assembly of the native heterodimers. J Biol Chem 265:1134–1138.

Lemanski LF. 1973. Morphology of developing heart in cardiac lethal mutant Mexican axolotls (*Ambystoma mexicanum*). Dev Biol 33:312–333.

Lemanski LF, Nakatsugawa M, Bhatia R, Erginel-Unaltuna N, Spinner BJ, Dube DK. 1996. A specific synthetic RNA promotes cardiac myofibrillogenesis in the Mexican axolotl. Biochem Biophys Res Commun 229:974–981.

Lin JJ-C, Helfman DM, Hughes SH, Chou C-S. 1985. Tropomyosin isoforms in chicken embryo fibroblasts. Purification, characterization and changes in Rouse sarcoma virus-transformed cells. J Cell Biol 100:692–703.

Lin JJ-C, Warren KS, Wamboldt DD, Wang T, Lin JL-C. 1997. Tropomyosin isoforms in nonmuscle cells. Int Rev Cytol 170:1–38.

Luque EA, Lemanski LF, Dube DK. 1994. Molecular cloning, sequencing and expression of an isoform of cardiac alpha-tropomyosin from the Mexican axolotl (*Ambystoma mexicanum*). Biochem Biophys Res Commun 203: 319–325.

Luque EA, Spinner BJ, Dube S, Dube DK, Lemanski LF. 1997. Differential expression of a novel isoform of alpha-tropomyosin in cardiac and skeletal muscle of the Mexican axolotl (*Ambystoma mexicanum*). Gene 185: 175–185.

MacLeod AR, Talbot K, Smillie LB, Houlker C. 1987. Characterization of a cDNA defining a gene family encoding Tm30pl, a human fibroblast tropomyosin. J Mol Biol 194:1–10.

Moore PB, Lemanski LF. 1982. Quantitation of tropomyosin by radioimmunoassay in developing hearts of cardiac mutant axolotls, *Ambystoma mexicanum*. J Muscle Res Cell Motil 3:161–167.

Needleman SB, Wunsch CD. 1970. A general method applicable to the search for similarities in the amino acid sequence of two proteins. J Mol Biol 48:443–453.

Ordahl CP. 1992. Developmental regulation of sarcomeric gene expression. Dev Biol 26:145–168.

Pieples K, Wieczorek DF. 2000. Tropomyosin 3 increases striated muscle isoform diversity. Biochemistry 39:8291–8297.

Pittenger MF, Kazzaz JA, Helfman DM. 1994. Functional properties of non-muscle tropomyosin isoforms. Curr Opin Cell Biol 6:96–104.

Prasad GL, Fuldner RA, Cooper HL. 1993. Expression of transduced tropomyosin I cDNA suppresses neoplastic growth of cells transformed by the ras oncogene. Proc Natl Acad Sci USA 90:7039–7043.

Sambrook I, Fritsch EF, Maniatis T. 1989. Molecular cloning: a laboratory manual, 2nd edition. Cold Spring Harbor, NY: Cold Spring Harbor Laboratory Press.

Schevzov G, Lloyd C, Hailstones D, Gunning P. 1993. Differential regulation of tropomyosin isoform organization and gene expression in response to altered actin gene expression. J Cell Biol 121:811–821.

Smillie LB. 1979. Structure and function of tropomyosin from muscle and non-muscle sources. Trends Biochem Sci 4:151–155.

Starr C, Diaz JG, Lemanski LF. 1989. Analysis of actin and tropomyosin in hearts of cardiac mutant axolotls by two-dimensional gel electrophoresis, Western blots, and immunofluorescent microscopy. J Morphol 201:1–10.

Swofford DL. 1991. Phylogenetic analysis using parsimony version 3.05. Computer program distributed by the Illinois Natural History survey, Champaign, Illinois.

Vize PD, Hemmati-Brivanlou A, Harland RM, Melton DA. 1991. Assays for gene function in developing *Xenopus* embryos. Methods Cell Biol 36:368–387.

Wieczorek DF, Smith CWJ, Nadal-Ginard B. 1988. The rat α-tropomyosin gene generates a minimum of six different mRNAs coding for striated, smooth and nonmuscle isoforms by alternative splicing. Mol Cell Biol 8:679–694.

Zackson SL, Steinberg MS. 1986. Cranial neural crest cells exhibit directed migration on the pronephric duct pathway: further evidence for an in vivo adhesion gradient. Dev Biol 117:343–353.

Zajdel RW, McLean MD, Lemanski SL, Muthuchamy M, Wieczorek DF, Lemanski LF, Dube DK. 1998. Ectopic expression of tropomyosin promotes myofibrillogenesis in mutant axolotl hearts. Dev Dyn 213:412–420.

Zelphati O, Szoka FC, Jr. 1996. Mechanism of oligonucleotide release from cationic liposomes. Proc Natl Acad Sci USA 93:11493–11498.

Zot AS, Potter JD. 1987. Structural aspects of troponin-tropomyosin regulation of skeletal muscle contraction. Ann Rev Biophys Biophysical Chem 16:535–559.